Effects of spontaneously generated coherence on the pump-probe response of a Λ system

Sunish Menon[1] and G. S. Agarwal[1,2]
[1]*Physical Research Laboratory, Navrangpura, Ahmedabad 380 009, India*
[2]*Max-Plank-Institut Für Quantenoptik, 85748 Garching, Germany*
(Received 9 July 1997; revised manuscript received 18 November 1997)

Near-degenerate lower levels in a Λ system have an additional coherence term due to interaction with the vacuum of the radiation field. We report the effects of this *spontaneously generated coherence* on the formation of a trapped state in the presence of two coherent fields of arbitrary intensity. We show that such coherence preserves both electromagnetically induced transparency and coherent population trapping (CPT) phenomena. However, it changes the time scales associated with the formation of the CPT state, and brings about quantitative changes in the line profiles. We present a clear analytical explanation for our numerical results. We also report the dependence of line shapes on the relative phase between the two applied fields. [S1050-2947(98)10005-7]

PACS number(s): 42.50.Gy, 42.50.Ar, 42.50.Hz

I. INTRODUCTION

It is now well understood how the decay of a system of closely lying states induced by interaction with a common bath leads to new types of coherences [1–8]. These coherences modify, among other things, the line shapes of spontaneous emission. An early study of a V system consisting of two degenerate levels showed the possibility of coherent trapping in the excited state [1]. This system and its generalizations have been the subject of recent studies in connection with the production of quantum beats and probe absorption [4–6]. Javanainen [8] discussed the possibility of spontaneously generated coherence (SGC) effects in a Λ system. In particular, he examined the response of the Λ system to an external pump of arbitrary intensity, and demonstrated that the dark state could disappear in the presence of a strong spontaneously generated coherence. The existence of these coherence effects depends on the nonorthogonality of the two dipole matrix elements.

More explicitly, the basic equations describing spontaneous emission from an excited state to two close-lying lower states are given by [8] (Fig. 1 with $\vec{\varepsilon}_1 = \vec{\varepsilon}_2 = \vec{0}$)

$$\dot{\rho}_{11} = -2(\gamma_1+\gamma_2)\rho_{11}, \quad \dot{\rho}_{12} = -(\gamma_1+\gamma_2)\rho_{12},$$
$$\dot{\rho}_{22} = 2\gamma_2\rho_{11}, \quad \dot{\rho}_{13} = -(\gamma_1+\gamma_2)\rho_{13}, \tag{1}$$
$$\dot{\rho}_{33} = 2\gamma_1\rho_{11}, \quad \dot{\rho}_{23} = 2\sqrt{\gamma_1\gamma_2}\cos\theta\rho_{11}e^{i\Omega t}.$$

Here 2γ's represent the spontaneous emission rate, θ is the angle between the two induced dipole moments $\vec{d}_{12}$ and $\vec{d}_{13}$, and $\hbar\Omega$ is the energy spacing between the two ground levels. All the elements of ρ above, except ρ_{23}, have their usual dependence. It should be noted that only for small Ω are the effects of generated coherence between $|2\rangle$ and $|3\rangle$ important, as for large Ω the rapid oscillations in ρ_{23} will average out any such effects. While Javanainen examined the effects of such coherences on the response of the system to a single field of arbitrary intensity, we examine its effect on electromagnetically induced transparency (EIT) [9,10] and coherent population trapping (CPT) [11] phenomena.

The organization of this paper is as follows: In Sec. II, we present the effects of SGC on the absorption and dispersion line shapes. We show the existence of CPT even in the presence of SGC. In Sec. III, we study the approach to CPT, i.e., we study dynamical effects. In Sec. IV, we develop an analysis which explains the numerical results of Secs. II and III in a transparent manner. In Sec. V, we show the dependence of the line shapes on the relative phase between the pump and probe fields. Finally in Sec. VI, we discuss the kind of situations where SGC will be nonzero and connect to other recent works on this subject.

II. ABSORPTION AND DISPERSION LINE SHAPES IN PRESENCE OF SGC

We consider a Λ system driven by two coherent fields with amplitudes $\vec{\varepsilon}_1$ and $\vec{\varepsilon}_2$. Since the dipole moments are not orthogonal, we have to consider an arrangement where each field (pump and probe) acts only on one transition. This can be achieved by considering the case shown in Fig. 1, where the probe (pump) acts on the transition $|1\rangle \leftrightarrow |3\rangle$ ($|1\rangle \leftrightarrow |2\rangle$). In such case the density-matrix equation in the rotating-wave approximation will be

$$\dot{\rho}_{11} = -2(\gamma_1+\gamma_2)\rho_{11} + ig\rho_{31} + iG\rho_{21} - iG^*\rho_{12} - ig^*\rho_{13},$$
$$\dot{\rho}_{22} = 2\gamma_2\rho_{11} + iG^*\rho_{12} - iG\rho_{21},$$
$$\dot{\rho}_{33} = 2\gamma_1\rho_{11} + ig^*\rho_{13} - ig\rho_{31}, \tag{2}$$
$$\dot{\rho}_{12} = -(\gamma_1+\gamma_2+i\Delta_2)\rho_{12} + ig\rho_{32} - iG(\rho_{11}-\rho_{22}),$$
$$\dot{\rho}_{13} = -(\gamma_1+\gamma_2+i\Delta_1)\rho_{13} + iG\rho_{23} - ig(\rho_{11}-\rho_{33}),$$
$$\dot{\rho}_{23} = -i(\Delta_1-\Delta_2)\rho_{23} + 2\sqrt{\gamma_1\gamma_2}\cos\theta\eta\rho_{11} + iG^*\rho_{13} - ig\rho_{21},$$

where η will be zero (one) if the spontaneously generated coherence effect is ignored (included). Here the coupling coefficients are denoted as $G = \vec{d}_{12}\cdot\vec{\varepsilon}_2/\hbar$ and $g = \vec{d}_{13}\cdot\vec{\varepsilon}_1/\hbar$, i.e., $G = G_0\sin\theta$ and $g = g_0\sin\theta$, and the detunings are $\Delta_2 = W_{12} - w$ and $\Delta_1 = W_{13} - w$, where $\hbar W_{ij}$ is the energy separation between states $|i\rangle$ and $|j\rangle$. For simplicity we assume $\vec{d}\cdot\vec{\varepsilon}_i$ ($i=1,2$) to be real, and ignore the dephasing terms. The general steady-state analytical solution for ρ_{13} in all orders of probe and pump is

$$\rho_{13}=\frac{gG^2(\Delta_1-\Delta_2)[-g^2+\eta_0 gG-G^2+\Delta_1(\Delta_1-\Delta_2)+2i(\Delta_1-\Delta_2)]}{D}, \tag{3}$$

$$\begin{aligned}D=&[(g^2+G^2)^2(g^2-\eta_0 Gg+G^2)+(2g^2+2G^2-\eta_0 Gg)\\&\times(g^2-G^2)\Delta_2(\Delta_1-\Delta_2)+(4G^2+4g^2+4G^2g^2\\&+\eta_0 gG^3-2G^4+(g^2+G^2)\Delta_2^2)(\Delta_1-\Delta_2)^2\\&+2G^2\Delta_2(\Delta_1-\Delta_2)^3+G^2(\Delta_1-\Delta_2)^4],\end{aligned} \tag{4}$$

where $\eta_0=2\eta\cos\theta$, and we have set $\gamma_1=\gamma_2=\gamma$. All the parameters are reduced to dimensionless units by scaling with γ. For a weak probe ($g\ll G$),

$$\rho_{13}\approx\frac{-g(\Delta_1-\Delta_2)}{[G^2+(\Delta_1-\Delta_2)(2i-\Delta_1)]}, \tag{5}$$

which is independent of the spontaneously generated coherence parameter η. We also note that $\mathrm{Im}(\rho_{13})=0$ when $\Delta_1=\Delta_2$ for all values of η_0, as for the arrangement in Fig. 1, $G^2-\eta_0 Gg+g^2\neq 0$ (for $\theta=0$, both the fields are perpendicular to the dipoles). Thus coherent population trapping phenomena is preserved for all values of η_0. From Eq. (3), we also see that the line profiles will start showing significant deviations if the probe field becomes large, so as to saturate the transition. These features are demonstrated in Figs. 2 and 3. These scans correspond to changing of the separation Ω (Fig. 1). Note that $\mathrm{Im}(\rho_{13})=0$ at $\Delta_1=\Delta_2$ in all the cases. In Figs. 2 and 3, we also show for comparison the results when the spontaneously generated coherence term η is ignored. For large values of Δ_1-Δ_2, the difference between the two profiles disappear. This is because, as noted earlier, the effect is important only for small values of energy separation between $|2\rangle$ and $|3\rangle$. Similar results are obtained for unequal γ's.

III. EFFECTS OF SGC ON DYNAMICS

We also study the dynamic evolution of the system to the CPT state by solving equations (2) numerically with initial conditions $\rho_{11}=\rho_{22}=0$, $\rho_{33}=1$, and $\rho_{ij}=0$, for $i\neq j$. The time evolution of the ground-state coherence is shown in Fig. 4. We perform an eigenvalue analysis of the above resulting 8×8 matrix in Eqs. (2) to ascertain the time scales involved with both strong and weak probes. Typically, for $G=g=10\sin\theta$ and $\gamma_1=\gamma_2=1$, we diagonalize the matrix with (without) the parameter η. The eigenvalues are $-2.85+19.95i$, $-2.85-19.95i$, $-1.0-9.95i$, $-1.0-9.95i$, $-1.0+9.95i$, $-1.0+9.95i$, -1.99, -0.288 ($-2.5+19.9i$, $-2.5-19.9i$, $-1.0-9.95i$, $-1.0+9.95i$, $-1.0-9.95i$, $-1.0+9.95i$, -2.0, -0.99). It is observed that the lowest eigenvalue, which is inversely related to the time scale, reduces from -0.99 to -0.28 in the presence of spontaneously generated coherence, thus lengthening the time scale to evolve to the CPT state as shown in Fig. 4. For smaller probe strength ($g=0.1\sin\theta$) the lowest eigenvalue changes from -0.985 to -0.97, hardly affecting the time scale.

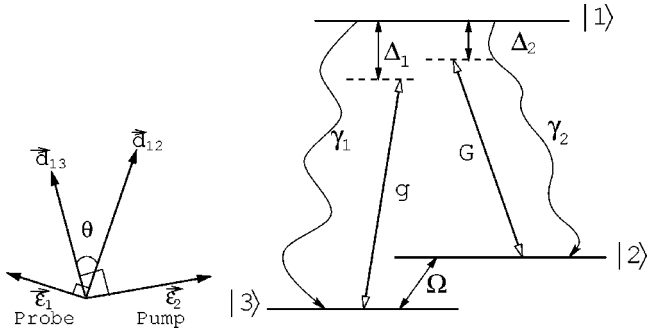

FIG. 1. Schematic diagram of a three-level Λ system driven by two coherent fields of equal frequency but with Rabi frequencies $2g$ (probe) and $2G$ (pump), respectively. The field polarizations are chosen so that one field drives only one transition.

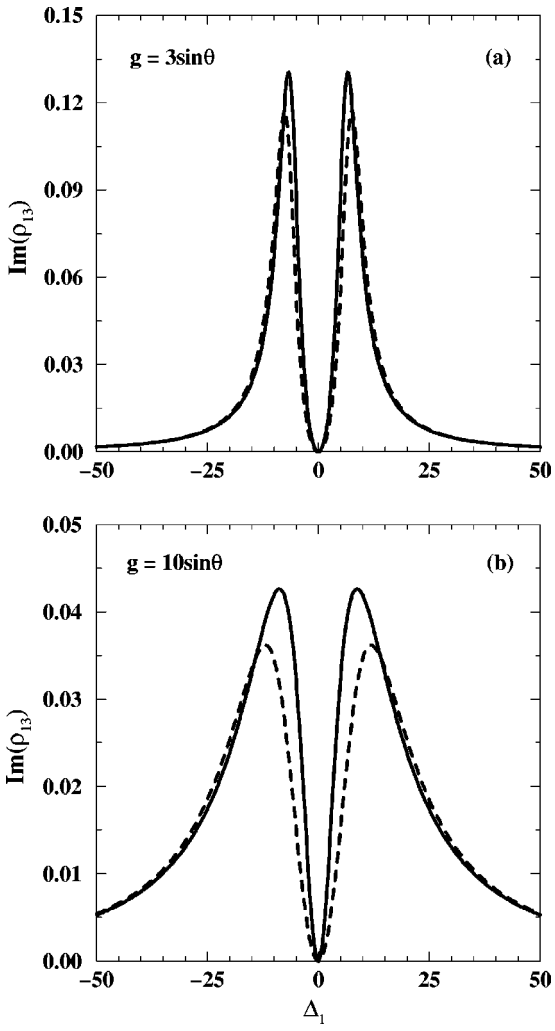

FIG. 2. Energy absorption from probe $\mathrm{Im}(\rho_{13})$ for $G=10\sin\theta$, $\Delta_2=0$, $\gamma_1=\gamma_2=1$, and $\theta=45°$. The solid (dashed) curve is with $\eta=1$ (0). The probe strengths are normalized to γ and are as given in the figures.

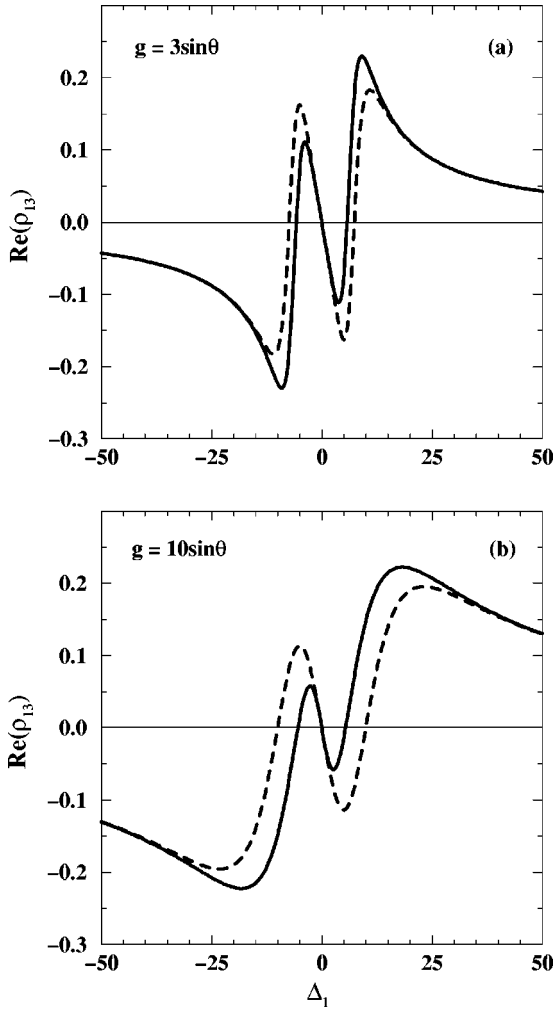

FIG. 3. Plots for $\mathrm{Re}(\rho_{13})$ as function of probe detuning. The parameters are the same as in Fig. 2.

IV. EXPLANATION OF NUMERICAL RESULTS

We now demonstrate how we can understand numerical results by analyzing the original density matrix equations (2) in a field-dependent basis given by

$$|1\rangle,\ \ |+\rangle=\frac{G|2\rangle+g|3\rangle}{F},\quad |-\rangle=\frac{g|2\rangle-G|3\rangle}{F}, \tag{6}$$

where $F=\sqrt{G^2+g^2}$. We assume the CPT condition $\Delta_1=\Delta_2$ throughout this section. Note that basis (6) is different from the dressed state basis which will also involve mixing of $|1\rangle$ and $|+\rangle$ states. For understanding the numerical results, basis (6) turns out to be useful. We can now transform the density matrix equations (2) using

$$\begin{aligned}
\rho_{++}&=(G^2\rho_{22}+g^2\rho_{33}+Gg\rho_{23}+Gg\rho_{32})/F^2,\\
\rho_{--}&=(g^2\rho_{22}+G^2\rho_{33}-Gg\rho_{23}-Gg\rho_{32})/F^2,\\
\rho_{1+}&=(G\rho_{12}+g\rho_{13})/F,\\
\rho_{1-}&=(g\rho_{12}-G\rho_{13})/F.
\end{aligned} \tag{7}$$

In the new basis, we obtain the equations

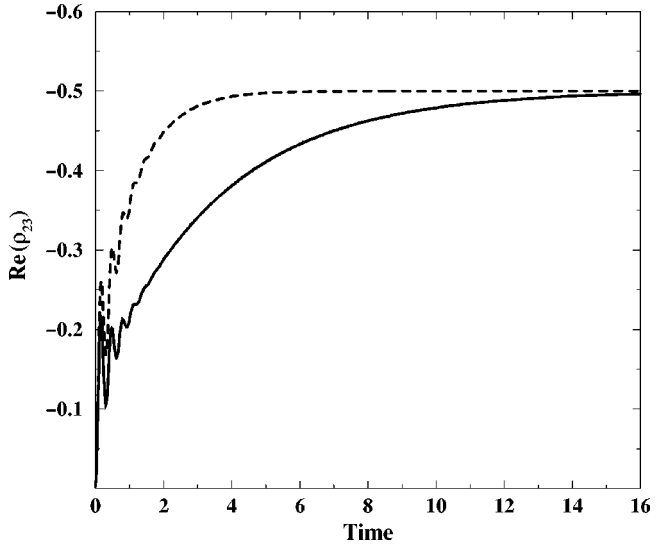

FIG. 4. Dynamic evolution of the system to the CPT state. The solid (dashed) curve is in the presence (absence) of the SGC parameter η. The parameters are $G=g=10\sin\theta$, $\Delta_1=\Delta_2=0$, $\gamma_1=\gamma_2=1$, and $\theta=45°$. Time is measured in units of γ^{-1}.

$$\begin{aligned}
\dot{\rho}_{11}&=-2\Gamma\rho_{11}+iF\rho_{+1}-iF\rho_{1+},\\
\dot{\rho}_{1+}&=-\Gamma\rho_{1+}+iF(\rho_{++}-\rho_{11}),\\
\dot{\rho}_{++}&=(\Gamma+\Gamma')\rho_{11}+iF\rho_{1+}-iF\rho_{+1},\\
\dot{\rho}_{--}&=(\Gamma-\Gamma')\rho_{11},\\
\dot{\rho}_{1-}&=-\Gamma\rho_{1-}+iF\rho_{+-},\\
\dot{\rho}_{+-}&=iF\rho_{1-}-\Gamma'\frac{(G^2-g^2)}{2Gg}\rho_{11},
\end{aligned} \tag{8}$$

where $\Gamma'=2\Gamma Gg\cos\theta\eta/(G^2+g^2)$. Equation (8) can be interpreted in term of the diagram shown in Fig. 5. We note that the CPT state $|-\rangle$ is populated at the rate Γ_{CPT}, where

$$\Gamma_{\mathrm{CPT}}=\Gamma\left(1-\frac{2Gg\cos\theta\eta}{G^2+g^2}\right). \tag{9}$$

It is important to see for the geometry considered in the Fig. 1 this rate of population of the CPT state can never be zero:

$$\Gamma_{\mathrm{CPT}}\neq 0. \tag{10}$$

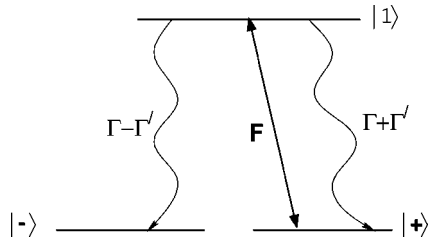

FIG. 5. Equivalent level scheme of Fig. 2 in the basis $|1\rangle$, $|+\rangle$, and $|-\rangle$. The population oscillates between the states $|1\rangle$ and $|+\rangle$, with an effective Rabi frequency F, and decays to the CPT state $|-\rangle$ at the rate Γ-Γ'.

Note further that the population is cycled between the levels $|1\rangle$ and $|+\rangle$ because of the effective pumping field $F \equiv \sqrt{G^2+g^2}$. It is clear from this physical picture that optical pumping would lead to the state $|-\rangle$, i.e., the CPT would occur.

This analysis also explains why Javanainen [8] found a very different result for the case of a single field. His case corresponds to setting $g=G$ and $\theta=0$, leading to $\Gamma_{\rm CPT}=0$. Thus the CPT state is not populated, and no optical pumping to this state occurs. In this case, one has a conservation law

$$\dot{\rho}_{--}=0. \tag{11}$$

Thus the final population in $|-\rangle$ state is the same as that given by the initial condition. The case considered by Javanainen is equivalent to that of a two-level system with states $|1\rangle$ and $|+\rangle$.

Finally, the above equations also enable us to understand the numerical results of Fig. 4. In the absence of SGC, $\Gamma'=0$, and the CPT state $|-\rangle$ is populated at a rate Γ, i.e., the CPT state is populated slowly in the presence of SGC. This is precisely what our numerical results of Fig. 4 show. The field dependence of Γ' can be borne in mind:

$$\Gamma'=\frac{2\Gamma\eta\cos\theta(g/G)}{1+(g/G)^2}. \tag{12}$$

Thus important changes in time scales would occur only when g and G are comparable.

V. PHASE-DEPENDENT ABSORPTION LINE SHAPES

The usual EIT experiments with well separated ground levels in a Λ system do not depend on the relative phase between the two applied fields. However, in the case of a closely spaced level, as our numerical simulation reveals, SGC makes the system quite sensitive to the relative phase between the two applied fields. Explicitly, we consider phases ϕ_2 and ϕ_1 of the pump and probe fields, respectively. Then one can rewrite the Rabi frequencies as $G\equiv Ge^{-i\phi_2}$ and $g\equiv ge^{-i\phi_1}$. Redefining the atomic variables in Eq. (2) as $\tilde{\rho}_{12}\equiv\rho_{12}e^{i\phi_2}$, $\tilde{\rho}_{13}\equiv\rho_{13}e^{i\phi_1}$, and $\tilde{\rho}_{23}\equiv\rho_{23}e^{i\Phi}$, where $\Phi=\phi_1-\phi_2$, we obtain equations for the redefined density-matrix elements $\tilde{\rho}_{ij}$ which are found to be identical to Eq. (2), with the SGC parameter η replaced by

$$\eta_\phi\equiv\eta e^{i\Phi}. \tag{13}$$

The absorption of the probe is now obtained from the imaginary part of $\tilde{\rho}_{13}$. Clearly as long as line shapes depend on the parameter η, they would also depend on the relative phase between the two fields. We display this dependence of the line shapes on the relative phase between the pump and probe fields in Fig. 6. It may also be noted that parameters like γ_1 and γ_2 are independent of the phases of the dipole matrix elements, whereas η depends on the phases of the two dipole matrix elements. The phase dependence of the line shapes is reminiscent of the phase dependence of the line shapes of spontaneous emission found by Martinez *et al.* [3].

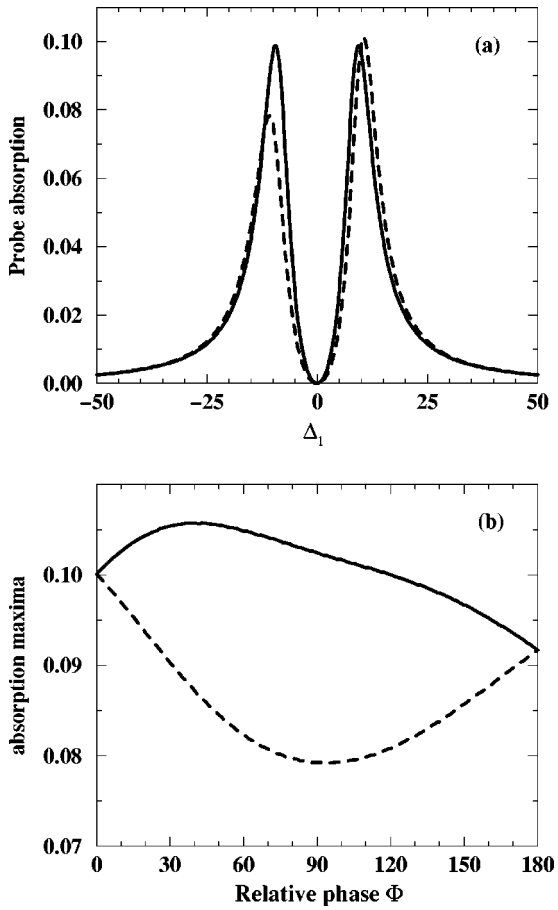

FIG. 6. Figures show the dependence of line profiles on the relative phase Φ between the two applied fields: (a) shows an appreciable difference in the line profiles corresponding to $\Phi=90°$ (dashed curve) and $\Phi=0°$ (solid curve), (b) normalized probe absorption maximas $(\text{peak abs.})_\Phi$ /$(\text{peak abs.})_{\Phi=0}$ as a function of Φ in the presence of SGC. The solid (dashed) curve is for maxima in the region $\Delta_1>0$ ($\Delta_1<0$). Other parameters are $G=10\sin\theta$, $g=3\sin\theta$, $\theta=45°$, and $\Delta_2=0.0$ for both (a) and (b).

VI. CONCLUSIONS

Before concluding, we discuss how to arrive at a situation where the dipole elements for the two optical transitions are nonorthogonal. Xia, Ye, and Xhu [5] considered the superposition of singlet and triplet states due to spin-orbit coupling in sodium dimers. This results in a series of coupled pairs of near-degenerate levels, each of them sharing singlet and triplet wave functions. These pairs generate nonorthogonal dipoles, and a suitable pair can be selected by tuning the frequency. Thus in their case the nonorthogonality was obtained from the mixing of the levels arising from internal fields [12]. One could also use external microwave fields to mix the levels, so as to achieve the nonorthogonality of the dipole matrix elements. It may be added that a large body of current papers [3–6,13] on interference effects uses situations where the two dipole matrix elements are nonorthogonal.

In conclusion, we have shown that (a) CPT is preserved in all cases, but the time taken to reach CPT is more when both the fields are of the same order. (b) The response of the system to first order in the probe field, but to all orders in the

pump, does not depend on the spontaneously generated coherence parameter η. (c) The line profiles depend strongly on the coherence parameter η if the probe field is strong. Here the width of the CPT structure goes down if $\eta \neq 0$, which also results in a shifting of the peaks close to the center. (d) The difference in line profiles due to a relative phase between the two applied fields is also discussed. We also give an analytical explanation for our numerical results.

[1] G. S. Agarwal, *Quantum Optics*, Springer Tracts in Modern Physics Vol. 70 (Springer, Berlin, 1974), p. 95.

[2] D. A. Cardimona, M. G. Raymer, and C. R. Stroud Jr., J. Phys. B **15**, 55 (1982).

[3] M. A. G. Martinez, P. R. Herczfeld, C. Samuels, L. M. Narducci, and C. H. Keitel, Phys. Rev. A **55**, 4483 (1997). We note here that an inclusion of the polarization of the radiation fields would imply that the interference term of this paper occurs only if the dipole matrix elements for the two optical transitions are nonorthogonal.

[4] A. Imamoğlu, Phys. Rev. A **40**, 2835 (1989); M. O. Scully, S. Y. Zhu, and A. Gavrielides, Phys. Rev. Lett. **62**, 2813 (1989); S. Y. Zhu, R. C. F. Chan, and C. P. Lee, Phys. Rev. A **52**, 710 (1995); G. C. Hegerfeldt and M. B. Plenio, *ibid.* **46**, 373 (1992).

[5] H. R. Xia, C. Y. Ye, and S. Y. Zhu, Phys. Rev. Lett. **77**, 1032 (1996).

[6] P. Zhou and S. Swain, Phys. Rev. Lett. **78**, 832 (1997); P. Zhou and S. Swain, Phys. Rev. A **56**, 3011 (1997).

[7] G. S. Agarwal, Phys. Rev. A **55**, 2457 (1997).

[8] J. Javanainen, Europhys. Lett. **17**, 407 (1992).

[9] S. E. Harris, J. E. Field, and A. Imamoğlu, Phys. Rev. Lett. **64**, 1107 (1990).

[10] K. Hakuta, L. Marmet, and B. P. Stoicheff, Phys. Rev. Lett. **66**, 596 (1991); K. J. Boller, A. Imamoğlu, and S. E. Harris, *ibid.* **66**, 2593 (1991); M. Xiao, Y. Li, S. Jin, and J. Gea-Banacloche, *ibid.* **74**, 666 (1995); J. Gea-Banacloche, Y. Li, S. Jin, and M. Xiao, Phys. Rev. A **51**, 576 (1995); Y. Li and M. Xiao, *ibid.* **51**, 4959 (1995); D. J. Fulton, S. Shepherd, R. Moseley, B. D. Sinclair, and M. H. Dunn, *ibid.* **52**, 2303 (1995).

[11] For a recent review article, see E. Arimondo in *Progress in Optics*, edited by E. Wolf (North-Holland, Amsterdam, 1996), Vol. XXXV, p. 257, and references therein.

[12] Similar types of interference effects have been discussed in quantum-well structures: M. O. Scully (unpublished); see also H. Schmidt and A. Imamoğlu, Opt. Commun. **131**, 333 (1996).

[13] H. Lee, P. Polyrikin, M. O. Scully, and S. Y. Zhu, Phys. Rev. A **55**, 4454 (1997); S. Y. Zhu and M. O. Scully, Phys. Rev. Lett. **76**, 388 (1996).